



Cite this: *RSC Adv.*, 2016, 6, 56738

# Discovery of novel chemical scaffolds as RhoA inhibitors using virtual screening, synthesis, and bioactivity evaluation†

Chao Zhang,<sup>ab</sup> Hui-Jie Wang,<sup>ab</sup> Qi-Chao Bao,<sup>ab</sup> Jin-Lei Bian,<sup>ab</sup> Ying-Rui Yang,<sup>ab</sup> Qi-Dong You<sup>\*ab</sup> and Xiao-Li Xu<sup>\*ab</sup>

RhoA has been implicated in diverse cellular functions and is a potential cancer therapeutic target. Through virtual screening, we have identified a RhoA inhibitor, **DDO-5701**. **DDO-5701** has an affinity to RhoA at the micromolar level *in vitro*. By structural modifications, considering the binding activity and synthesis ease of **DDO-5701**, 17 compounds were designed and synthesized accordingly. Among these compounds, 4 compounds (**DDO-5713**, **DDO-5714**, **DDO-5715**, **DDO-5716**) exhibited higher RhoA inhibition activities than **DDO-5701**, while **DDO-5716** can effectively reverse the functions of breast cancer cells regulated by RhoA. Thus, the rationally designed small molecule inhibitor of RhoA (**DDO-5716**) is useful for studying the physiological and pathological roles of Rho GTPase. However, **DDO-5701** is an approved drug – proglumide, which makes it and its derived compound **DDO-5716** more likely to be well tolerated in humans and could quickly lead to further clinical development.

Received 3rd May 2016  
Accepted 27th May 2016

DOI: 10.1039/c6ra11398b

[www.rsc.org/advances](http://www.rsc.org/advances)

## 1. Introduction

RhoA is a small GTPase, belonging to the Ras super family. RhoA and its downstream effectors are instrumental in regulating cytoskeleton organization, gene expression, cell cycle progression, cell motility, and other cellular processes.<sup>1–3</sup> RhoA GTPases shuttle between an inactive GDP-bound and an active GTP-bound form, which allows it to carry out its cellular functions through its downstream effectors mDIA and ROCKs.<sup>4–7</sup> Hyper-expressed or activated RhoA is involved in cancer progression of several human tumours.<sup>8–10</sup> Particularly, RhoA deficiency suppresses the invasive type of breast cancer cells,<sup>11,12</sup> whereas elevated RhoA activity can induce breast cancer cell migration, invasion and metastasis.<sup>13</sup> RhoA has been suggested to serve as a potential therapeutic target of breast cancer.

The inactive form of RhoA can turn to the active form of RhoA in response to a variety of upstream signals, such as growth factors, cytokines, adhesion molecules and cell intrinsic oncogenic cues. Within the RhoA signaling module, two strategies of intervention have been proposed for effective suppression of RhoA activities. One strategy is targeting GTP binding sites to compete with GTP leading to RhoA inactivation,<sup>14</sup> while

the other strategy is targeting the GEF–RhoA interactive surface essential for the guanine nucleotide exchange reaction also leading to RhoA inactivation.<sup>15,16</sup> To date, both strategies have led to effective small molecular compounds targeting RhoA (Fig. 1).

In the current work, we initiated a program aimed at seeking the small molecule RhoA inhibitors. By using a docking-based virtual screening approach in conjunction with fluorescence polarization (FP) determination, one novel small molecule RhoA binder (hit) (**DDO-5701**) has been discovered and selected as the starting point for further structural optimization. In total, 17 new compounds have been designed, synthesized, and tested with biological assays. Finally, four compounds (**DDO-5713**, **DDO-5714**, **DDO-5715** and **DDO-5716**) were found to show higher RhoA inhibition activities compared to **DDO-5701**, and compound **DDO-5716** was further selected to study the

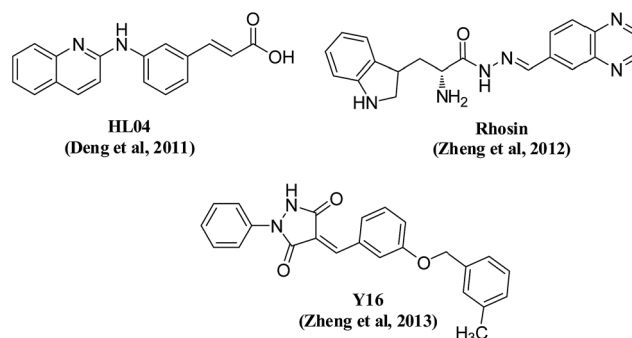


Fig. 1 Representative structures of known inhibitors of RhoA.

<sup>a</sup>State Key Laboratory of Natural Medicines and Jiangsu Key Laboratory of Drug Design and Optimization, China Pharmaceutical University, Nanjing, 210009, China. E-mail: youqd@163.com; xuxiao\_li@126.com

<sup>b</sup>Department of Medicinal Chemistry, School of Pharmacy, China Pharmaceutical University, Nanjing, 210009, China

† Electronic supplementary information (ESI) available. See DOI: 10.1039/c6ra11398b

mechanism of this structure of small molecular compounds targeting RhoA. It is useful for studying the physiological function of the RhoA subfamily GTPases and for determining the therapeutic potential of Rho targeting in pathological conditions.

**DDO-5701** is an approved drug called proglumide, which initially has only been used as a drug to reduce gastric motility and pancreatic secretion in patients. Proglumide acts as an antagonist on the cholecystokinin receptor blocking pancreatic amylase secretion and gall bladder contraction initiated by gastrin.<sup>17</sup> In addition, proglumide has been found to have anti-tumor properties *in vitro* and *in vivo* in the past few decades.<sup>18–22</sup> Proglumide was regarded as a gastrin receptor blocking agent, which could decrease gastrin-derived cell proliferation of gastrointestinal tumors. However, our findings demonstrated that proglumide binding to RhoA, which leads to RhoA inactivity, may be the main cause of the exhibited anti-tumor activity of proglumide.

## 2. Methodology

### 2.1. Computation

**2.1.1 Compound database preparation.** A subset of the MayBridge and US drug collection database of commercially available compounds was used, and the bank of 63 000 compounds was prepared using Prepare Ligands module and Minimize Ligands module in Discovery Studio 4.0 (DS 4.0). Multiple conformations of each compound were generated through the Diverse Conformation Generation protocol with an energy threshold of 20 kcal mol<sup>-1</sup> and a maximum of 255 conformations.

**2.1.2 Virtual screening.** Docking is a conventional structure-based virtual screening method. The molecular docking studies were performed using two different programs: LigandFit/DS 4.0 and Genetic Optimization for Ligand Docking (GOLD 5.1, Cambridge Crystallographic Data Center). In the present study, a crystal (PDB ID: 1KMQ) was employed for docking studies. Residues around GNP (radius 8 Å) were defined as the active site. All other parameters were set as default. The docking was terminated when the top ten solutions attained root-mean-square deviation (RMSD) values within 1.5 Å. A similarity search was undertaken using the program Diverse Subset (MOE 2014.09).

### 2.2. Biology

**2.2.1 Recombinant protein production.** Recombinant human RhoA (residues 1–193) was expressed in the *E. coli* DH5 $\alpha$  strain as GST fusions by using the pGEX-2T vector (addgene, Cat no. 12202). The N-terminal tagged GST fusion protein was purified by glutathione–agarose affinity chromatography.

**2.2.2 Fluorescence polarization (FP).** We consulted a published paper and made some changes to contribute to our FP method.<sup>23</sup> A total of 1  $\mu$ M GST-tagged RhoA protein (vector was obtained from addgene, Cat no. 12202) was incubated with a 40 nM BODIPY FL-tagged GTP $\gamma$ S fluorescence probe in FP buffer (20 mM Tris, 150 mM NaCl, 10 mM MgCl<sub>2</sub>, 10% glycerine,

0.01% IGEPAL, 1 mM freshly DTT, pH = 7.5). Compounds were added in the FP buffer at the indicated concentrations. For control wells, equal DMSO from test compounds was added into the wells. After incubation at RT for 1 hour, mP values were measured by the SpectraMax Paradigm Microplate Reader (Molecular Devices).

**2.2.3 Thermal shift assay.** The thermal shift assay was performed according to the instruction of the Thermal shift dye kit (ThermoFisher, Cat no. 4461146). Briefly, 2.6  $\mu$ L of GST-tagged RhoA protein and 2.5  $\mu$ L of dye were first dispensed into each well of a 96-well microplate. Then 0.5  $\mu$ L of the test compound suspended in 14.5  $\mu$ L of buffer containing 10 mM MgCl<sub>2</sub> were dispensed into each well to generate test ligands at 50  $\mu$ M in an assay volume of 20  $\mu$ L. For control wells, equal DMSO from test compounds was added into the wells. The resulting amount of protein utilized is usually 1.5  $\mu$ M. The plate was subsequently heated from 25 °C to 99 °C in the StepOne™plus Real-Time PCR System (Applied Biosystems). Fluorescent intensity was recorded in this process. Protein Thermal Shift™ Software v1.0 (Applied Biosystems) was utilized to analyze recording data from StepOne plus system.

**2.2.4 p50RhoGAP assay.** Inorganic phosphate produced as a result of GTPase activity was measured by using a p50RhoGAP assay (Cytoskeleton, Cat no. BK105) and absorbance-based detection method. Briefly, (His)<sub>6</sub>-tagged RhoA was preloaded with GTP or **DDO-5701** and incubated in the reaction buffer (provided in the kit) for 20 min at 37 °C. p50GAP was then added for an additional 20 min at 37 °C. Following a 10 min incubation in CytoPhos reagent (Cytoskeleton), inorganic phosphate was detected at 650 nm.

**2.2.5 Isothermal titration calorimetry (ITC).** An ITC200 calorimeter (Malvern) was used to carry out the ITC experiment. 300  $\mu$ L of GST-tagged RhoA protein was inserted into the sample cell at a concentration of 30  $\mu$ M in a buffer containing 20 mM Tris, pH 7.4, 150 mM NaCl and 10 mM MgCl<sub>2</sub>. The syringe was filled with test compound in the same buffer condition. Two microliter aliquots of a 300  $\mu$ M solution were titrated into the sample cell at 25 °C. 180 s intervals and a stirring speed of 1000 rpm were used for the whole procedure of the injection. In addition, the first 0.5 mL of the ligand solution was titrated to prevent initial interference. All the data obtained from the experiment including the association constant ( $K_a$   $\frac{1}{4}$   $1/K_d$ ), enthalpy value (DH) and entropy value (DS) were analyzed by the Origin software package.

**2.2.6 Endogenous Rho GTPase activity assay.** MCF7 cells were grown in log phase in a 10 cm dish, which were starved in serum-free medium in the presence or absence of **DDO-5701** and **DDO-5716** at indicated concentrations for 24 hours and were subsequently stimulated with LPA for 10 min at a 50 ng mL<sup>-1</sup> concentration. MCF7 cells were lysed in lysis buffer containing 50 mM Tris, pH = 7.4, 10 mM MgCl<sub>2</sub>, 0.5 M NaCl, 2% IGEPAL. Lysates were clarified and the protein concentrations were normalized. The GTP bound RhoA in the lysates was pulled down by rhotekin RBD beads (Cytoskeleton, Cat no. RT02) and was measured by a respective anti-RhoA (Cytoskeleton, Cat no. ARH04) western blot. RhoA downstream protein phospho-MLC/MLC in the lysates was measured by an anti-p-MLC and

anti-MLC (Cell Signaling, Cat no. 3672, 3674, respectively) western blot.

**2.2.7 Immunofluorescence.** After overnight serum starvation in the presence or absence of **DDO-5701** and **DDO-5716** at the indicated concentration, MCF7 cells were treated with LPA at  $50 \text{ ng mL}^{-1}$  for 10 min. The cells were washed twice with cold PBS and fixed for 30 min with 4% (w/v) formaldehyde at RT temperature. Then the fixed cells were washed three times with PBS containing 0.1% Triton X-100, followed by washing three times with PBS. The fixed cells were blocked with 5% (w/v) BSA, and stained with an appropriate primary antibody (anti-vinculin, 1 : 200 Abcam, CA, Cat no. ab73412; anti-Ki67, 1 : 50, Abcam, CA, Cat no. ab16667), followed by Fluor488-conjugated secondary antibody (Invitrogen, CA, Cat no. A21202). For the stress fiber formation assay, the cells were stained with rhodamine phalloidin for 30 min (Cytoskeleton, Cat no. PHDR1). The coverslips were mounted in Vectashield mounting medium with DAPI. The fluorescence images were obtained with an Olympus fluorescence microscope.

**2.2.8 Cell proliferation assay.** MCF7 cells and MDA-MB-231 cells were seeded in 96-well plates at an initial density of 5000 cells per well and **DDO-5701** or **DDO-5716** treatment was performed on the second day. On the following days,  $10 \mu\text{L}$  of thiazolyl blue (MTT) was added to each well and incubated at  $37^\circ\text{C}$  for 4 h. Then the medium was removed carefully and  $150 \mu\text{L}$  of DMSO was added followed by gentle shaking. The optical density of the released color was read at 570 nm.

### 3. Results and discussions

#### 3.1. Database screening for potential RhoA inhibitors

To identify novel RhoA inhibitors, we built a simple screening protocol to carry out the virtual screening (Fig. 2). The MayBridge and US drug collection database containing 63 000 compounds were first searched using the “LigandFit” protocol in DS. 6300 hits (10% of the ranked compounds) were obtained and further screened using GOLD docking. After the filtering, we received 315 hits (5% of the ranked compounds) for the next studies. Because this number included a large degree of similar compounds and PAINS (pan-assay interference compounds),

with respect to scaffold and chemical class, a diversity analysis was undertaken using the program Diverse Subset (MOE 2014.09) and subsequently followed with visual inspection to avoid the potential of PAINS. Finally, 34 molecules were selected.

#### 3.2. Biological assay of the hit molecules

To characterize the inhibition of RhoA by the 34 molecules, a fluorescence polarization (FP) competitive binding assay was used to measure the binding affinity to RhoA (represented as  $\text{IC}_{50}$  values). We developed our FP methods based on a reported method with some changes.<sup>23</sup> In our FP experiments, we only used recombinant RhoA protein instead of the RhoA protein and LARG protein combination reported in that paper, in order to evaluate the molecules’ affinities for competing with GTP. Among the 34 molecules, we found compound **34 (DDO-5701)** had the highest affinity to RhoA ( $\text{IC}_{50} = 0.699 \pm 0.12 \mu\text{M}$ ) and we chose this compound as a hit to further test its affinity to RhoA (Fig. 3).

The thermal shift assay (TSA) operates on the principle that ligand binding alters the thermal stability of proteins.<sup>24,25</sup> TSA provides a measurement of a temperature shift and its setup allows one to monitor protein denaturation upon heating *via* fluorescent-based detection. A fluorescent dye based probe is used that preferentially binds the hydrophobic regions of a protein, which are increasingly exposed during protein denaturation. When coupled to a real-time PCR setup, monitoring the change in fluorescence provides a thermal melting curve or thermogram. The mid-point of the melting curve, *i.e.*, the temperature at which 50% of the protein has denatured, is designated as the melting temperature,  $T_m$ , and is a measure of the protein’s inherent thermal stability.<sup>26</sup> A ligand bound to a protein, *e.g.* to its active site, has the propensity to increase its thermal stability (and hence its  $T_m$ ) through newly formed ligand–protein interactions. In this manner, a melting curve is generated, the  $T_m$  determined, and the changes in  $T_m$  ( $\Delta T_m$ ) induced by prospective binding ligands can be calculated. **DDO-5701** exhibited  $\Delta T_m$  values ranging from  $3.68\text{--}4.08^\circ\text{C}$  at a  $25 \mu\text{M}$  concentration, which demonstrated that **DDO-5701** had an affinity to RhoA (Fig. 4A).

RhoA has a weak GTPase activity and is hard to detect, while p50RhoGAP can increase the GTPase activity of RhoA.<sup>27</sup> We had utilized a commercial kit to detect RhoA GTPase activity through a simple absorbance based detection method. We found that increased concentrations of **DDO-5701** ranging from  $25\text{--}100 \mu\text{M}$  could compete with preloaded GTP on RhoA and reduces GTP hydrolysis by purified recombinant RhoA protein *in vitro* (Fig. 4B). Taken together, **DDO-5701** had an affinity binding to RhoA and was a potential hit for RhoA inhibitors.

#### 3.3. Design of new derivatives based on hit compound **DDO-5701** and precursor evaluation

In order to optimize the structure of **DDO-5701**, the docked pose of the identified hit was analysed within the RhoA binding pocket. The general molecular orientation and the spatial

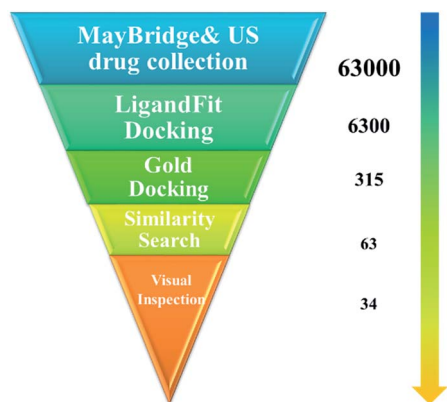


Fig. 2 The screening protocol that was applied to RhoA inhibitors.

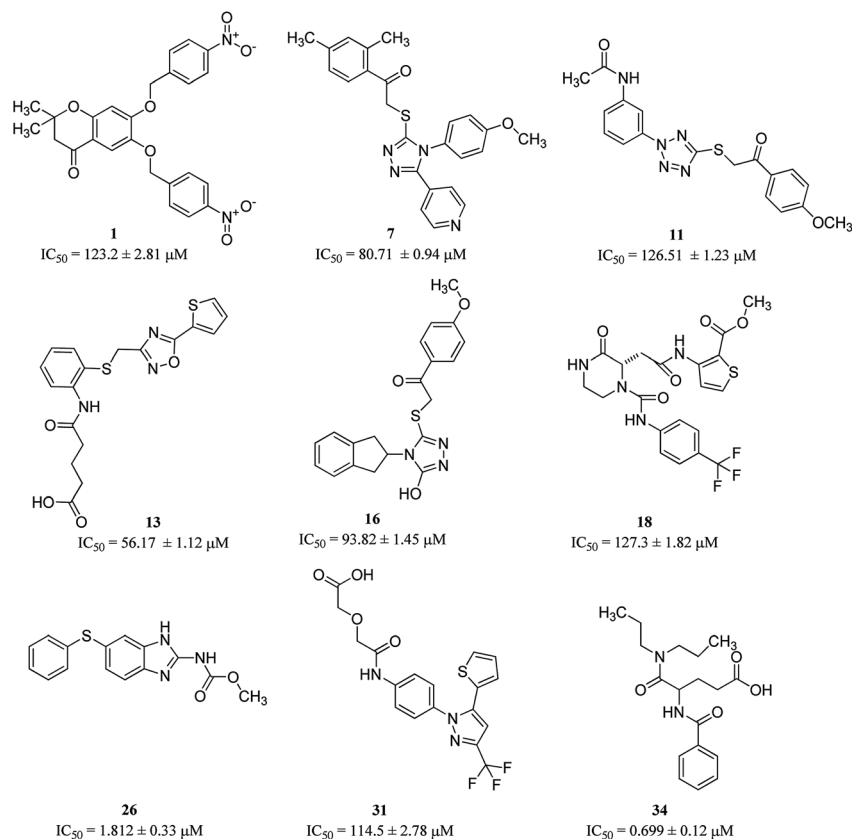


Fig. 3 Nine ligands were found by VS from the database.

location of the chemical features of **DDO-5701** are shown in Fig. 5C and D. The binding mode of the co-crystal GNP of RhoA is shown in Fig. 5A and B, which is featured by the triphosphate group forming complex hydrogen bonds with the backbone of the surrounding residues as well as a salt bridge with Lys18 for further stabilizing the binding pose of GNP.<sup>25</sup> The general molecular orientation and the spatial location of the chemical features of **DDO-5701** were similar to that of GNP. It was found

that the carboxyl group of **DDO-5701** could bind firmly to the Thr19 and Gly17 residues by hydrogen bonding interactions, which was similar to GNP in complex with RhoA. In addition, the carboxyl group could also form a strong salt bridge with Lys18. Moreover, the propanediamine group could occupy the guanine site formed by Pyr34, Thr19 and Thr37. And the carboxyl attached to the propanediamine could form another hydrogen bond with Thr19.

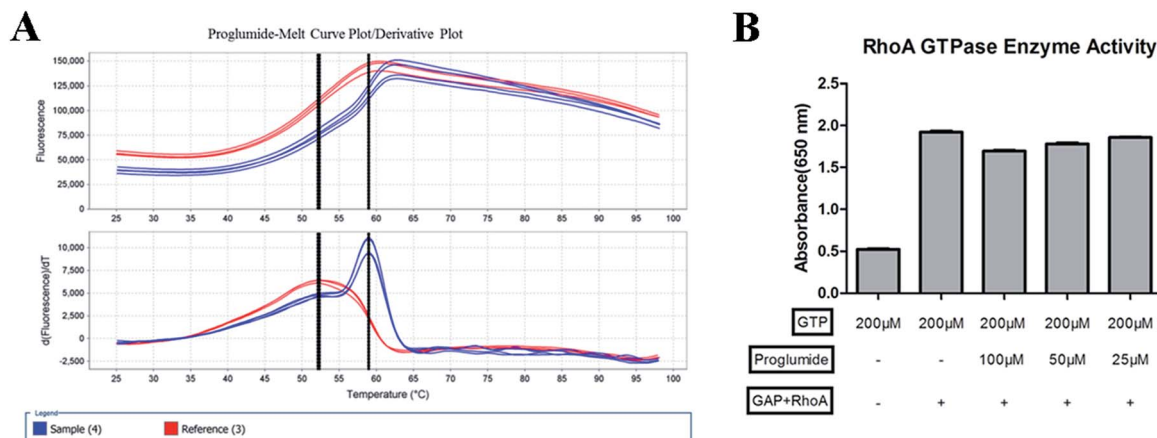


Fig. 4 (A) **DDO-5701** has affinity to RhoA detected by TSA. **DDO-5701** has exhibited  $\Delta T_m$  values ranging from 3.68–4.08 °C at a 25 μM concentration. (B) **DDO-5701** reduced RhoA GTPase activity demonstrated by the p50RhoGAP assay.

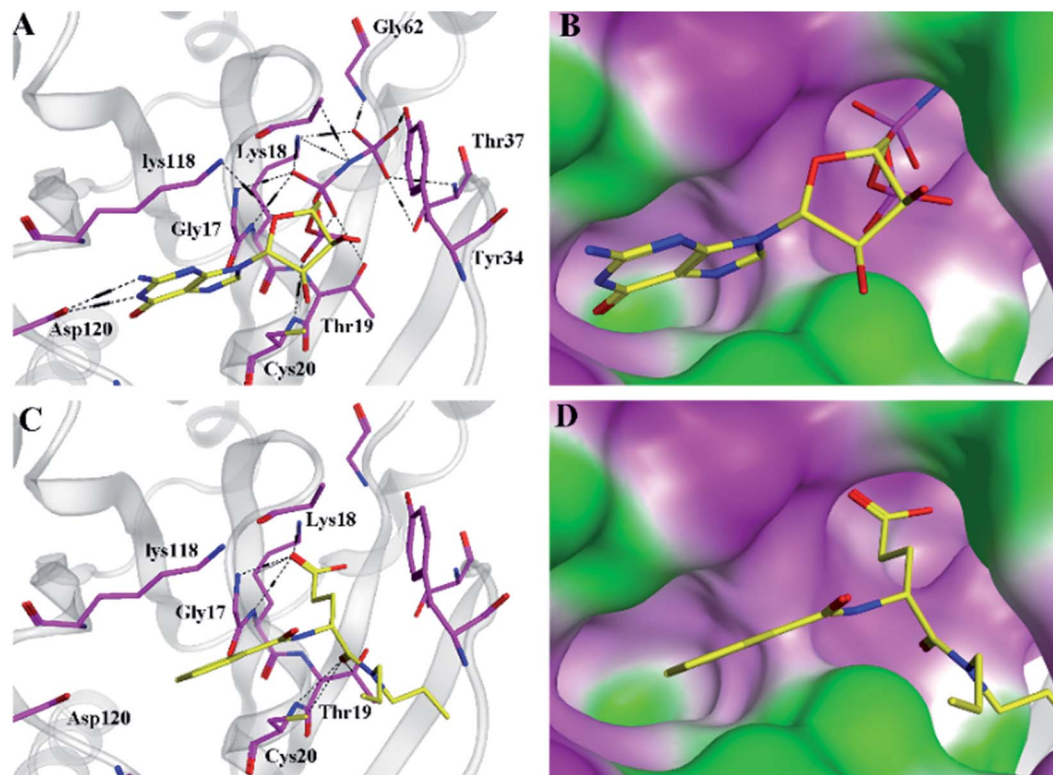


Fig. 5 The binding site of GNP (A and B) and DDO-5701 (C and D) with RhoA. The binding pattern was generated from the cocrystal structure (PDB code: 1KMQ) depicted using MOE 2014.09. The carbon atoms of GNP and DDO-5701 and the key residues in the active site of RhoA were colored in yellow and purple, respectively.

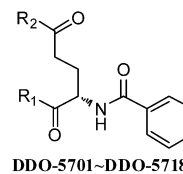
On the basis of the binding mode of the hit compound **DDO-5701** with RhoA, we designed two series of derivatives of **DDO-5701** to further study the detailed structure activity relationship (SAR) (**DDO-5702–DDO-5718**) and several more potent inhibitors were identified (**DDO-5713–DDO-5716**). We used the FP competitive binding assay to measure the ability of these derivatives for the binding affinity to RhoA. As shown in Table 1, compound **DDO-5702–DDO-5709** and **DDO-5718** displayed lower activity, indicating the carboxy group was necessary for inhibitors of RhoA. The phenomenon could be attributed to the H-bond and salt bridge disappearance between carboxy and RhoA. Notably, compound **DDO-5716** was the most potent inhibitor with an  $IC_{50}$  of  $0.318 \pm 0.11 \mu\text{M}$ . **DDO-5716** could be a promising RhoA inhibitor for further studies.

### 3.4. Chemistry

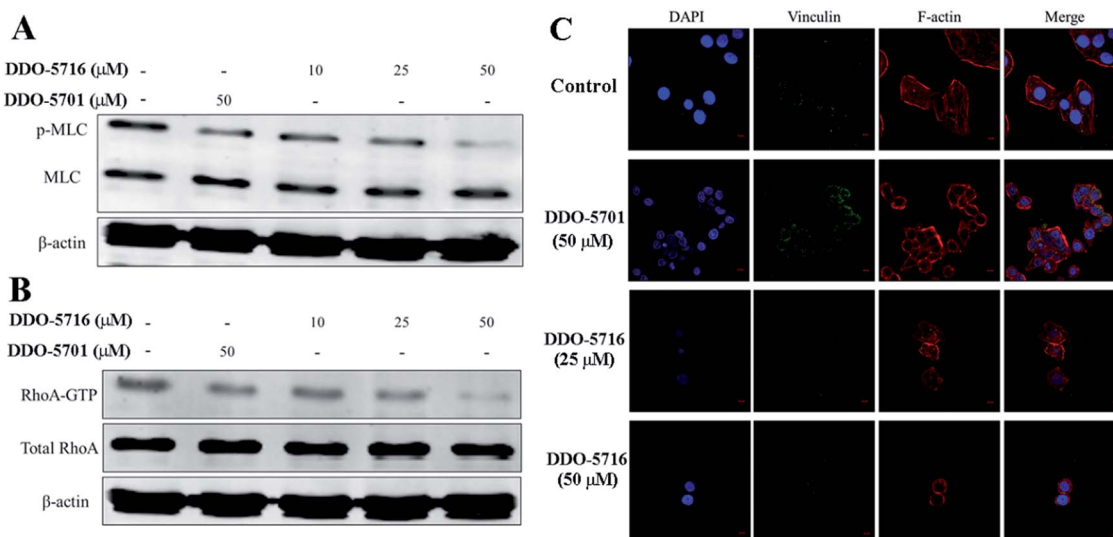
The synthesis routes used to prepare compounds **DDO-5702–DDO-5718** are shown in Scheme 1. Compound **DDO-5702**, starting from commercially available glutamic acid-5-methyl ester (**1**) and benzoyl chloride (**2**), provided the product in 85.1% yield. Then, the target compounds **DDO-5703–DDO-5709** were obtained through the coupling reaction of acid **DDO-5702** with different amines, carried out using 1-(3-dimethylaminopropyl)-3-ethylcarbodiimide hydrochloride (EDCI)/1-hydroxybenzotriazole (HOBt) in  $\text{CH}_2\text{Cl}_2$  (Scheme 1). Hydrolysis of compound **DDO-5702** and **DDO-5703–DDO-5709** using sodium hydroxide provided the product **DDO-5717** and

Table 1 Inhibition of RhoA by compounds **DDO-5701–DDO-5718**

Cpd	R <sup>1</sup>	R <sup>2</sup>	IC <sub>50</sub> (μM)
<b>DDO-5702</b>	OH	OMe	80.71 ± 1.31
<b>DDO-5703</b>	Et <sub>2</sub> N	OMe	85.22 ± 1.41
<b>DDO-5704</b>	EtNH	OMe	123.1 ± 1.36
<b>DDO-5705</b>	Me <sub>2</sub> N	OMe	131.3 ± 0.82
<b>DDO-5706</b>	Piperidin-1-yl	OMe	35.22 ± 1.18
<b>DDO-5707</b>	<i>p</i> -Br-PhNH	OMe	23.95 ± 1.26
<b>DDO-5708</b>	<i>p</i> -Cl-PhNH	OMe	24.45 ± 1.31
<b>DDO-5709</b>	<i>p</i> -MeO-PhNH	OMe	21.49 ± 0.99
<b>DDO-5710</b>	Et <sub>2</sub> N	OH	0.904 ± 0.11
<b>DDO-5711</b>	EtNH	OH	1.373 ± 0.21
<b>DDO-5712</b>	Me <sub>2</sub> N	OH	1.794 ± 0.35
<b>DDO-5713</b>	Piperidin-1-yl	OH	0.561 ± 0.33
<b>DDO-5714</b>	<i>p</i> -Br-PhNH	OH	0.339 ± 0.21
<b>DDO-5715</b>	<i>p</i> -Cl-PhNH	OH	0.414 ± 0.12
<b>DDO-5716</b>	<i>p</i> -MeO-PhNH	OH	0.318 ± 0.11
<b>DDO-5717</b>	OH	OH	1.273 ± 0.24
<b>DDO-5718</b>	Et <sub>2</sub> N	Et <sub>2</sub> N	208.8 ± 2.14
<b>DDO-5701</b>	( <i>n</i> -Pr) <sub>2</sub> N	OH	0.712 ± 0.07







**Fig. 7** (A) DDO-5716 treatment affects signaling downstream of RhoA. Western blots are of p-MLC/MLC and relevant controls of MCF7 cells treated with DDO-5716 or DDO-5701 at indicated concentrations (B) DDO-5716 can reduce RhoA-GTP formation. Blotting of the respective total-cell lysates was carried out in parallel. Results shown are representative of three independent experiments. (C) Effect of DDO-5716 on cell stress fiber and focal complex assembly. The cells were stained with rhodamine-phalloidin for F-actin (red) and anti-vinculin for focal adhesion complexes (green). Images shown are representative of more than 100 cells examined. DDO-5716 can reduce stress fiber and focal complex formation.

which we derived from DDO-5701 exhibited a better affinity than DDO-5701 to RhoA protein *in vitro*.

Elevated RhoA activities have been associated with cancer cell hyperproliferative and invasive behaviors.<sup>28</sup> Next, we investigated whether DDO-5716 was effective in suppressing RhoA activity in MCF7 cells. MCF7 cells grown in serum-free media were treated with DDO-5716 or DDO-5701 (as the

positive control) in different concentrations, followed by stimulation with LPA. As shown in Fig. 7B, DDO-5716 strongly inhibited RhoA-GTP formation in a dose-dependent manner, indicating endogenous RhoA activity inhibition at MCF7 cells. To evaluate the ability of DDO-5716 to inhibit RhoA-mediated cell functions, we next examined actin cytoskeleton structures of cells stimulated by serum or LPA in the absence or presence

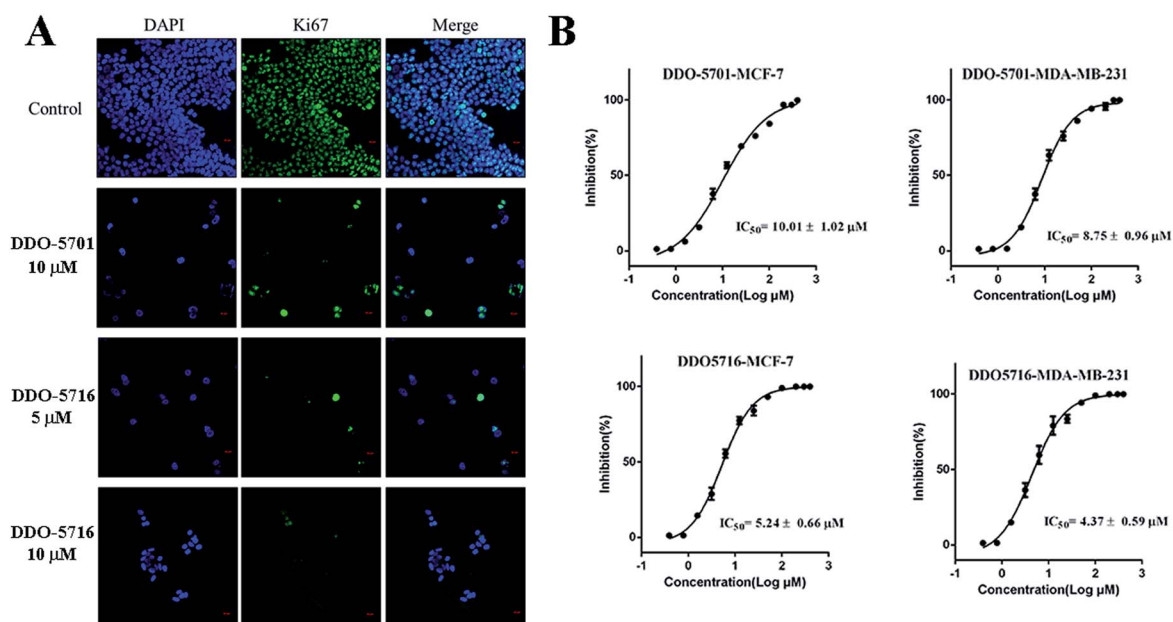


**Fig. 8** DDO-5716 inhibited breast cancer cell proliferation. (A) Cell proliferation was measured by Ki67 immunostaining. Cells were stained with anti-Ki67 antibodies to detect cell proliferation ability (green), and with DAPI, to detect nuclei (blue).  $n = 5$ . (B) The  $\text{IC}_{50}$  values of DDO-5701 and DDO-5716's inhibition of cell growth were measured by using the thiazolyl blue assay at MCF7 and MDA-MB-231 cell lines.  $n = 10$ , bar: SD.

of **DDO-5716**. Fig. 7C shows that in the presence of 25  $\mu\text{M}$  **DDO-5716**, stress fiber and formation of the MCF7 cells were significantly reduced, and at the 50  $\mu\text{M}$  concentration, both the stress fiber and focal complex formation of the MCF7 cells were significantly reduced, while at the 50  $\mu\text{M}$  concentration of **DDO-5701**, we only observed stress fiber formation reducing. Moreover, Fig. 7A shows **DDO-5716** dose-dependently reduced p-MLC activities, while p-MLC indicated actin-myosin contraction.<sup>29,30</sup> Given the implicated role of Rho activity in actin cytoskeleton organization and adhesion,<sup>31</sup> these results indicate that **DDO-5716** is active in inhibiting RhoA-mediated cellular events.

To assess the cellular effect of **DDO-5716**, we performed a cell proliferation assay using the MTT assay and Ki67 staining immunofluorescence. As shown in Fig. 8B, **DDO-5716** showed more effective inhibition of growth of MCF7 and MDA-MB-231 ( $\text{IC}_{50} = 5.24 \pm 0.66 \mu\text{M}$ ,  $\text{IC}_{50} = 4.37 \pm 0.39 \mu\text{M}$ , respectively) than **DDO-5701** ( $\text{IC}_{50} = 10.01 \pm 1.02 \mu\text{M}$ ,  $\text{IC}_{50} = 8.75 \pm 0.96 \mu\text{M}$ , respectively). In the presence of 5  $\mu\text{M}$  **DDO-5716**, Ki67 staining was significantly reduced, which indicated reduced cell proliferation, while Ki67 staining was reduced at a 10  $\mu\text{M}$  concentration of **DDO-5701** (Fig. 8A). These results indicated that **DDO-5716** was effective in targeting RhoA mediated breast cancer cell proliferation. The underlying mechanism as to why proglumide shows anti-cancer properties remains poorly understood. Proglumide was initially used as an anti-tumor agent through its blocking of the cholecystokinin A/B receptor ( $\text{CCK}\alpha/\beta$ ) or gastrin receptor. Our findings indicated that proglumide exhibited anti-tumor activity in breast cancer cells, which did not show  $\text{CCK}\alpha/\beta$  and gastrin receptor expression. The effect of cell proliferation inhibition of **DDO-5701** (proglumide) may be the result of its interaction with other receptor targets, but taken together with our results, proglumide might reduce breast cancer cell proliferation largely due to its binding to RhoA and leading to RhoA-GTP formation decreasing.

## 4. Conclusions

In summary, we have identified a lead small molecule inhibitor targeting RhoA by using a structure-based virtual screening approach in conjunction with chemical synthesis and bioassays. The lead molecule **DDO-5701** had an affinity to RhoA *in vitro* by several measured methods. On the basis of the structure of the lead compound **DDO-5701**, preliminary chemical modifications were performed. In total, 17 compounds have been synthesized and tested with biological assays, 11 compounds of them are new compounds (**DDO-5704**–**DDO-5709**, **DDO-5712**, **DDO-5714**–**DDO-5716**, **DDO-5718**). Finally, 4 compounds (**DDO-5713**, **DDO-5714**, **DDO-5715** and **DDO-5716**) were found to exhibit higher RhoA inhibition activities than **DDO-5701**. Among these compounds, **DDO-5716**, which showed the highest RhoA inhibition activity, had exhibited a better affinity to RhoA than **DDO-5701** and could effectively reverse the functions of breast cancer cells regulated by RhoA. Moreover, molecular binding models give rational explanations about SARs, which are in good agreement with pharmacological results. Thus, **DDO-5701** constitutes a series of small molecule inhibitors of

RhoA that is useful in the study of the physiological role of RhoA and for tackling RhoA-mediated pathologies.

## Acknowledgements

This work is supported by the project 81230078, 81502990 and 81573346 of National Natural Science Foundation of China; 2013ZX09402102-001-005 and 2014ZX09507002-005-015 of the National Major Science and Technology Project of China (Innovation and Development of New Drugs); Specialized Research Fund for the Doctoral Program of Higher Education (SRFDP, 20130096110002); A Project Funded by the Priority Academic Program Development of Jiangsu Higher Education Institutions; A project BK20150691 of Natural Science Foundation of Jiangsu Province; 2016ZPY016 of the Fundamental Research Funds for the Central Universities. This work is supported by the Project Program of State Key Laboratory of Natural Medicines, China Pharmaceutical University (No. SKLNMZZCX201611).

## References

- 1 S. Etienne-Manneville and A. Hall, *Nature*, 2002, **420**, 629–635.
- 2 A. J. Ridley, *Trends Cell Biol.*, 2001, **11**, 471–477.
- 3 I. M. Zohn, S. L. Campbell, R. Khosravi-Far, K. L. Rossman and C. J. Der, *Oncogene*, 1998, **17**, 1415–1438.
- 4 R. H. Insall and L. M. Machesky, *Dev. Cell*, 2009, **17**, 310–322.
- 5 O. Pertz, L. Hodgson, R. L. Klemke and K. M. Hahn, *Nature*, 2006, **440**, 1069–1072.
- 6 K. Riento and A. J. Ridley, *Nat. Rev. Mol. Cell Biol.*, 2003, **4**, 446–456.
- 7 R. A. Worthylake and K. Burridge, *J. Biol. Chem.*, 2003, **278**, 13578–13584.
- 8 A. Bellizzi, A. Mangia, A. Chiriatti, S. Petroni, M. Quaranta, F. Schittulli, A. Malfettone, R. A. Cardone, A. Paradiso and S. J. Reshkin, *Int. J. Mol. Med.*, 2008, **22**, 25–31.
- 9 A. Faried, L. S. Faried, N. Usman, H. Kato and H. Kuwano, *Ann. Surg. Oncol.*, 2007, **14**, 3593–3601.
- 10 A. Horiuchi, T. Imai, C. Wang, S. Ohira, Y. Feng, T. Nikaido and I. Konishi, *Lab. Invest.*, 2003, **83**, 861–870.
- 11 J. Y. Pille, C. Denoyelle, J. Varet, J. R. Bertrand, J. Soria, P. Opolon, H. Lu, L. L. Pritchard, J. P. Vannier, C. Malvy, C. Soria and H. Li, *Mol. Ther.*, 2005, **11**, 267–274.
- 12 C. H. Chan, S. W. Lee, C. F. Li, J. Wang, W. L. Yang, C. Y. Wu, J. Wu, K. I. Nakayama, H. Y. Kang, H. Y. Huang, M. C. Hung, P. P. Pandolfi and H. K. Lin, *Nat. Cell Biol.*, 2010, **12**, 457–467.
- 13 D. M. Brantley-Sieders, G. Zhuang, D. Hicks, W. B. Fang, Y. Hwang, J. M. Cates, K. Coffman, D. Jackson, E. Bruckheimer, R. S. Muraoka-Cook and J. Chen, *J. Clin. Invest.*, 2008, **118**, 64–78.
- 14 J. Deng, E. Feng, S. Ma, Y. Zhang, X. Liu, H. Li, H. Huang, J. Zhu, W. Zhu, X. Shen, L. Miao, H. Liu, H. Jiang and J. Li, *J. Med. Chem.*, 2011, **54**, 4508–4522.

- 15 X. Shang, F. Marchioni, N. Sipes, C. R. Evelyn, M. Jerabek-Willemsen, S. Duhr, W. Seibel, M. Wortman and Y. Zheng, *Chem. Biol.*, 2012, **19**, 699–710.
- 16 X. Shang, F. Marchioni, C. R. Evelyn, N. Sipes, X. Zhou, W. Seibel, M. Wortman and Y. Zheng, *Proc. Natl. Acad. Sci. U. S. A.*, 2013, **110**, 3155–3160.
- 17 E. Vijayan and S. M. McCann, *Brain Res. Bull.*, 1986, **16**, 533–536.
- 18 P. Singh, S. Le, R. D. Beauchamp, C. M. Townsend Jr and J. C. Thompson, *Cancer Res.*, 1987, **47**, 5000–5004.
- 19 G. Melen-Mucha, H. Lawnicka and S. Mucha, *Endokrynol. Pol.*, 2005, **56**, 933–938.
- 20 H. Wang, Q. Ni, Y. Zhang, Z. Yue, Q. Zhang and L. Hou, *Chin. J. Surg.*, 1999, **37**, 341–343.
- 21 G. Melen-Mucha, *Neoplasma*, 2001, **48**, 133–138.
- 22 S. Mauss, C. Niederau and K. J. Hengels, *Anticancer Res.*, 1994, **14**, 215–220.
- 23 C. R. Evelyn, T. Ferng, R. J. Rojas, M. J. Larsen, J. Sondek and R. R. Neubig, *J. Biomol. Screening*, 2009, **14**, 161–172.
- 24 M. W. Pantoliano, E. C. Petrella, J. D. Kwasnoski, V. S. Lobanov, J. Myslik, E. Graf, T. Carver, E. Asel, B. A. Springer, P. Lane and F. R. Salemme, *J. Biomol. Screening*, 2001, **6**, 429–440.
- 25 M. C. Lo, A. Aulabaugh, G. Jin, R. Cowling, J. Bard, M. Malamas and G. Ellestad, *Anal. Biochem.*, 2004, **332**, 153–159.
- 26 F. H. Niesen, H. Berglund and M. Vedadi, *Nat. Protoc.*, 2007, **2**, 2212–2221.
- 27 A. Bernards and J. Settleman, *Trends Cell Biol.*, 2004, **14**, 377–385.
- 28 E. Sahai and C. J. Marshall, *Nat. Rev. Cancer*, 2002, **2**, 133–142.
- 29 M. Amano, M. Ito, K. Kimura, Y. Fukata, K. Chihara, T. Nakano, Y. Matsuura and K. Kaibuchi, *J. Biol. Chem.*, 1996, **271**, 20246–20249.
- 30 K. Kimura, M. Ito, M. Amano, K. Chihara, Y. Fukata, M. Nakafuku, B. Yamamori, J. Feng, T. Nakano, K. Okawa, A. Iwamatsu and K. Kaibuchi, *Science*, 1996, **273**, 245–248.
- 31 A. Hall, *Science*, 1998, **279**, 509–514.